

International Journal of Modern Physics A  
 © World Scientific Publishing Company

## Magic square and Dirac flavor neutrino mass matrix

Yuta Hyodo

*Course of Physics, Graduate School of Science, Tokai University,  
 4-1-1 Kitakaname, Hiratsuka, Kanagawa 259-1292, Japan  
 0CSNM017@mail.u-tokai.ac.jp*

Teruyuki Kitabayashi

*Department of Physics, Tokai University,  
 4-1-1 Kitakaname, Hiratsuka, Kanagawa 259-1292, Japan  
 teruyuki@tokai-u.jp*

Received Day Month Year

Revised Day Month Year

The magic texture is one of the successful textures of the flavor neutrino mass matrix for the Majorana type neutrinos. The name “magic” is inspired by the nature of the magic square. We estimate the compatibility of the magic square with the Dirac, instead of the Majorana, flavor neutrino mass matrix. It turned out that some parts of the nature of the magic square are appeared approximately in the Dirac flavor neutrino mass matrix and the magic squares prefer the normal mass ordering rather than the inverted mass ordering for the Dirac neutrinos.

PACS numbers:14.60.Pq

### 1. Introduction

Understanding the nature of the flavor structure of elementary particles is one of the long-term problems in particle physics and cosmology.<sup>1,2</sup> Many texture ansatz to solve the flavor puzzle are proposed, such as tri-bi maximal texture,<sup>3–5</sup> texture zeros,<sup>6–41</sup>  $\mu - \tau$  symmetric texture<sup>42–62</sup> and textures under  $A_n$  as well as  $S_n$  symmetries.<sup>63</sup>

So-called *magic texture* is one of the textures of the flavor neutrino mass matrix for Majorana type neutrinos.<sup>64,65</sup> The magic texture is parametrized as

$$M = \begin{pmatrix} a & b & c \\ b & d & a+c-d \\ c & a+c-d & b-c+d \end{pmatrix}. \quad (1)$$

The applications of the magic texture have been studied for texture zeros of flavor neutrino mass matrix,<sup>66</sup> with two simple extensions<sup>67</sup> and for baryon asymmetry of the Universe.<sup>68</sup>

The name “magic” is inspired by the nature of the *magic square*.<sup>69</sup> A magic square of order  $n$  is a  $n \times n$  square grid filled with distinct natural numbers. Each cell contains a number in the range  $1, 2, \dots, n^2$ . The sum of the numbers in each row, each column and diagonal is equal. For example, a magic square of order 3 is schematically shown as

$$\begin{array}{|c|c|c|} \hline 2 & 7 & 6 \\ \hline 9 & 5 & 1 \\ \hline 4 & 3 & 8 \\ \hline \end{array} \leftarrow 15 \quad \begin{array}{|c|c|c|} \hline 2 & 7 & 6 \\ \hline 9 & 5 & 1 \\ \hline 4 & 3 & 8 \\ \hline \end{array} \leftarrow 15 \quad \begin{array}{|c|c|c|} \hline 2 & 7 & 6 \\ \hline 9 & 5 & 1 \\ \hline 4 & 3 & 8 \\ \hline \end{array} \leftarrow 15$$

↗ ↑ ↑ ↑ ↘  
15 15 15 15 15

(2)

where the sum (which is called magic constant or magic sum) is fifteen. The magic texture in Eq.(1) has a part of the nature of magic square, e.g., the sum of the elements in each row and each column is equal to  $a + b + c$ .

In this paper, we estimate the compatibility of the magic square with the Dirac, instead of the Majorana, flavor neutrino mass matrix by numerical calculations. We show that some parts of the nature of the magic square are appeared approximately in the Dirac flavor neutrino mass matrix. Moreover, as the main conclusion of this paper, we demonstrate that the magic squares prefer the normal mass ordering rather than the inverted mass ordering for the Dirac neutrinos.

This paper is organized as follows. In Section.2, ten types of magic square for the Dirac neutrinos are defined. In Section.3, the magic nature of the Dirac flavor neutrino mass matrix is estimated. Section 4 is devoted to a summary.

## 2. Classification

For a matrix

$$\begin{pmatrix} a & b & c \\ d & e & f \\ g & h & i \end{pmatrix} \leftarrow S_1 \quad \begin{pmatrix} a & b & c \\ d & e & f \\ g & h & i \end{pmatrix} \leftarrow S_2 \quad \begin{pmatrix} a & b & c \\ d & e & f \\ g & h & i \end{pmatrix} \leftarrow S_3$$

↗ ↑ ↑ ↑ ↘  
 $T'$      $S_4$   $S_5$   $S_6$      $T$

(3)

we define the following eight sums

$$\begin{aligned} S_1 &= a + b + c, & S_2 &= d + e + f, & S_3 &= g + h + i, \\ S_4 &= a + d + g, & S_5 &= b + e + h, & S_6 &= c + f + i, \\ T &= a + e + i, & T' &= c + e + g, \end{aligned} \quad (4)$$

and the following ten types of magic square for the Dirac neutrinos in the from of the  $3 \times 3$  matrix.

**Type-I:** The exact magic square (we call it type-I magic square) should satisfy the following requirement

$$S_1 = S_2 = S_3 = S_4 = S_5 = S_6 = T = T'. \quad (5)$$

In this case, the standard deviation should vanish:

$$sd_I = \sqrt{\frac{\sum_{i=1}^6 (S_i - \bar{S})^2 + (T - \bar{S})^2 + (T' - \bar{S})^2}{8}}, \quad (6)$$

where

$$\bar{S} = (S_1 + S_2 + S_3 + S_4 + S_5 + S_6 + T + T')/8, \quad (7)$$

is the average of the sums  $S_1, S_2, \dots, S_6, T$  and  $T'$ . For example, in the case of order 3 magic square

$$\begin{pmatrix} 2 & 7 & 6 \\ 9 & 5 & 1 \\ 4 & 3 & 8 \end{pmatrix}, \quad (8)$$

the sums

$$S_1 = S_2 = S_3 = S_4 = S_5 = S_6 = T = T' = 15, \quad (9)$$

and the average  $\bar{S} = 15$  are obtained and the standard deviation becomes  $sd_I = 0$ . Moreover, we obtain the vanishing standard deviation for the following decimal magic square:

$$\begin{pmatrix} 0.2 & 0.7 & 0.6 \\ 0.9 & 0.5 & 0.1 \\ 0.4 & 0.3 & 0.8 \end{pmatrix}. \quad (10)$$

Indeed, the sums of this decimal magic square

$$S_1 = S_2 = S_3 = S_4 = S_5 = S_6 = T = T' = 1.5, \quad (11)$$

and the average  $\bar{S} = 1.5$  are obtained and the standard deviation becomes  $sd_I = 0$ .

The standard deviation  $sd_I$  is a good number to show that whether a matrix has the nature of the exact type-I magic square or not; however, the standard deviation is not good number for our purpose in this paper. For example, the matrix

$$\begin{pmatrix} 2+1 & 7 & 6 \\ 9 & 5 & 1 \\ 4 & 3 & 8 \end{pmatrix}, \quad (12)$$

and

$$\begin{pmatrix} 0.2+0.1 & 0.7 & 0.6 \\ 0.9 & 0.5 & 0.1 \\ 0.4 & 0.3 & 0.8 \end{pmatrix}, \quad (13)$$

have a small perturbation for the type-I magic square in the (1,1) element. Because the requirement of the type-I magic square is only the relation of  $S_1 = S_2 = S_3 =$

$S_4 = S_5 = S_6 = T = T'$ , these two matrices are same level of type-I magic square; however, the standard deviations of the matrices in Eq.(12) and Eq.(13) are 0.484 and 0.0484, respectively.

We define the *magic index* for the type-I magic square as follows

$$s_I = \sqrt{\frac{\sum_{i=1}^6 (\frac{S_i}{S} - 1)^2 + (\frac{T}{S} - 1)^2 + (\frac{T'}{S} - 1)^2}{8}}. \quad (14)$$

The magic index  $s_I$  of the matrices in Eq.(12) and Eq.(13) are same as 0.0315.

The small magic index of a matrix means the matrix is much compatible with the magic square.

**Type-II:** If we relax the requirement of the exact magic square in Eq.(5), we can define the quasi-magic squares. Omitting the trace  $T$  in the exact magic requirement in Eq.(5), we have a new requirement

$$S_1 = S_2 = S_3 = S_4 = S_5 = S_6 = T', \quad (15)$$

for a matrix. We call a matrix with the requirement of Eq.(15) the type-II magic square. For the type-II magic square, we define the following magic index

$$s_{II} = \sqrt{\frac{\sum_{i=1}^6 (\frac{S_i}{S} - 1)^2 + (\frac{T'}{S} - 1)^2}{7}}, \quad (16)$$

where

$$\bar{S} = (S_1 + S_2 + S_3 + S_4 + S_5 + S_6 + T')/7. \quad (17)$$

**Type-III:** Omitting the sum  $T'$  in the exact magic constraint in Eq.(5), we have other new requirement

$$S_1 = S_2 = S_3 = S_4 = S_5 = S_6 = T, \quad (18)$$

for a matrix. We call a matrix with the requirement of Eq.(18) the type-III magic square and we define the following type-III magic index

$$s_{III} = \sqrt{\frac{\sum_{i=1}^6 (\frac{S_i}{S} - 1)^2 + (\frac{T}{S} - 1)^2}{7}}, \quad (19)$$

where

$$\bar{S} = (S_1 + S_2 + S_3 + S_4 + S_5 + S_6 + T)/7. \quad (20)$$

**Type-IV:** We define the type-IV magic square by omitting the sum  $T'$  and trace  $T$  in the exact magic requirement in Eq.(5). In this case, the requirement becomes

$$S_1 = S_2 = S_3 = S_4 = S_5 = S_6, \quad (21)$$

and we define the following type-IV magic index

$$s_{\text{IV}} = \sqrt{\frac{\sum_{i=1}^6 (\frac{S_i}{S} - 1)^2}{6}}, \quad (22)$$

where

$$\bar{S} = (S_1 + S_2 + S_3 + S_4 + S_5 + S_6)/6. \quad (23)$$

We note that the type-I,-II,-III and -IV magic squares for the Dirac neutrinos are naive extensions of the magic texture of the Majorana neutrino mass matrix in Eq.(1). Especially, the type-IV magic square is the most straight extension of the magic texture for Majorana neutrinos in Eq.(1).

**Type-V, -VI, -VII, -VIII, -XI and -X:** We add more scenarios by omitting the one of the sum in  $\{S_1, S_2, \dots, S_6\}$ . Namely, we define the type-V magic square with the following requirement (by omitting  $S_1$ )

$$S_2 = S_3 = S_4 = S_5 = S_6 = T = T', \quad (24)$$

and the type-V magic index

$$s_V = \sqrt{\frac{\sum_{i=2}^6 (\frac{S_i}{S} - 1)^2 + (\frac{T}{S} - 1)^2 + (\frac{T'}{S} - 1)^2}{7}}, \quad (25)$$

where

$$\bar{S} = (S_2 + S_3 + S_4 + S_5 + S_6 + T + T')/7. \quad (26)$$

Similarly, we define more five types of magic square with the following requirements

- $S_1 = S_3 = S_4 = S_5 = S_6 = T = T'$  : type-VI (by omitting  $S_2$ )
- $S_1 = S_2 = S_4 = S_5 = S_6 = T = T'$  : type-VII (by omitting  $S_3$ )
- $S_1 = S_2 = S_3 = S_5 = S_6 = T = T'$  : type-VIII (by omitting  $S_4$ )
- $S_1 = S_2 = S_3 = S_4 = S_6 = T = T'$  : type-IX (by omitting  $S_5$ )
- $S_1 = S_2 = S_3 = S_4 = S_5 = T = T'$  : type-X (by omitting  $S_6$ )

The magic indices  $s_{\text{VI}}$ ,  $s_{\text{VII}}$ ,  $\dots$   $s_{\text{X}}$  are defined by the same way for  $s_V$  in Eq.(25).

### 3. Magic square and Dirac neutrino mass matrix

In this section, first, we show the brief review of the Dirac neutrino mass matrix and the experimental data of the neutrinos. Then, we estimate the compatibility of the magic square with the Dirac flavor neutrino mass matrix by numerical calculations.

### 3.1. Neutrino mass matrix

The minimal flavor neutrino mass matrix for Dirac neutrinos is obtained by<sup>70</sup>

$$M = \begin{pmatrix} M_{ee} & M_{e\mu} & M_{e\tau} \\ M_{\mu e} & M_{\mu\mu} & M_{\mu\tau} \\ M_{\tau e} & M_{\tau\mu} & M_{\tau\tau} \end{pmatrix} = \begin{pmatrix} U_{e1}m_1 & U_{e2}m_2 & U_{e3}m_3 \\ U_{\mu 1}m_1 & U_{\mu 2}m_2 & U_{\mu 3}m_3 \\ U_{\tau 1}m_1 & U_{\tau 2}m_2 & U_{\tau 3}m_3 \end{pmatrix}, \quad (27)$$

where  $m_1, m_2$  and  $m_3$  denote the neutrino mass eigenstates and

$$\begin{aligned} U_{e1} &= c_{12}c_{13}, & U_{e2} &= s_{12}c_{13}, & U_{e3} &= s_{13}e^{-i\delta}, \\ U_{\mu 1} &= -s_{12}c_{23} - c_{12}s_{23}s_{13}e^{i\delta}, \\ U_{\mu 2} &= c_{12}c_{23} - s_{12}s_{23}s_{13}e^{i\delta}, & U_{\mu 3} &= s_{23}c_{13}, \\ U_{\tau 1} &= s_{12}s_{23} - c_{12}c_{23}s_{13}e^{i\delta}, \\ U_{\tau 2} &= -c_{12}s_{23} - s_{12}c_{23}s_{13}e^{i\delta}, & U_{\tau 3} &= c_{23}c_{13}, \end{aligned} \quad (28)$$

denote the elements of the Pontecorvo-Maki-Nakagawa-Sakata mixing matrix.<sup>71-74</sup> We used the abbreviations  $c_{ij} = \cos \theta_{ij}$  and  $s_{ij} = \sin \theta_{ij}$  ( $i, j = 1, 2, 3$ ). The Dirac CP phase is denoted by  $\delta$ . In this paper, we assume that the mass matrix of the charged leptons is diagonal and real.

A global analysis of current data shows the following the best-fit values of the squared mass differences  $\Delta m_{ij}^2 = m_i^2 - m_j^2$  and the mixing angles for the so-called normal mass ordering (NO),  $m_1 < m_2 < m_3$ , of the neutrinos:<sup>75</sup>

$$\begin{aligned} \frac{\Delta m_{21}^2}{10^{-5}\text{eV}^2} &= 7.39_{-0.20}^{+0.21} \quad (6.79 \rightarrow 8.01), \\ \frac{\Delta m_{31}^2}{10^{-3}\text{eV}^2} &= 2.528_{-0.031}^{+0.029} \quad (2.436 \rightarrow 2.618), \\ \theta_{12}/^\circ &= 33.82_{-0.76}^{+0.78} \quad (31.61 \rightarrow 36.27), \\ \theta_{23}/^\circ &= 48.6_{-1.4}^{+1.0} \quad (41.1 \rightarrow 51.3), \\ \theta_{13}/^\circ &= 8.60_{-0.13}^{+0.13} \quad (8.22 \rightarrow 8.98), \\ \delta/\circ &= 221_{-28}^{+39} \quad (144 \rightarrow 357), \end{aligned} \quad (29)$$

where the  $\pm$  denotes the  $1\sigma$  region and the parentheses denote the  $3\sigma$  region. On the other hands, for the so-called inverted mass ordering,  $m_3 < m_1 \lesssim m_2$ , we have

$$\begin{aligned} \frac{\Delta m_{21}^2}{10^{-5}\text{eV}^2} &= 7.39_{-0.20}^{+0.21} \quad (6.79 \rightarrow 8.01), \\ \frac{\Delta m_{32}^2}{10^{-3}\text{eV}^2} &= -2.510_{-0.031}^{+0.030} \quad (-2.601 \rightarrow -2.416), \\ \theta_{12}/^\circ &= 33.82_{-0.75}^{+0.78} \quad (31.61 \rightarrow 36.27), \\ \theta_{23}/^\circ &= 48.4_{-1.2}^{+1.0} \quad (41.4 \rightarrow 51.3), \\ \theta_{13}/^\circ &= 8.64_{-0.13}^{+0.12} \quad (8.26 \rightarrow 9.02), \\ \delta/\circ &= 282_{-25}^{+23} \quad (205 \rightarrow 348). \end{aligned} \quad (30)$$

Moreover, the following constraints

$$\sum m_i < 0.12 - 0.69 \text{ eV}, \quad (31)$$

from the cosmological observation of the cosmic microwave background radiation<sup>39, 76–79</sup> as well as

$$|M_{ee}| < 0.066 - 0.155 \text{ eV}, \quad (32)$$

from the neutrino less double beta decay experiments<sup>39, 80</sup> are obtained.

### 3.2. Numerical analysis

#### 3.2.1. Setup

To estimate the compatibility of the magic square with the Dirac flavor neutrino mass matrix by numerical calculations, we employ the following real matrix

$$\begin{pmatrix} a & b & c \\ d & e & f \\ g & h & i \end{pmatrix} = \begin{pmatrix} |M_{ee}| & |M_{e\mu}| & |M_{e\tau}| \\ |M_{\mu e}| & |M_{\mu\mu}| & |M_{\mu\tau}| \\ |M_{\tau e}| & |M_{\tau\mu}| & |M_{\tau\tau}| \end{pmatrix}, \quad (33)$$

instead of the complex Dirac mass matrix in Eq.(27).

In our numerical calculation, we require that the square mass differences  $\Delta m_{ij}^2$ , mixing angles  $\theta_{ij}$  and the Dirac CP violating phase  $\delta$  are varied within the  $3\sigma$  experimental ranges and the lightest neutrino mass is varied within  $0.001 - 0.1$  eV. We also require that the constraints  $|M_{ee}| < 0.155$  eV and  $\sum m_i < 0.241$  eV (TT, TE, EE+LowE+lensing<sup>40, 76</sup>) are satisfied.

In the following subsubsections, we show the result from the numerical calculations for the ten types of magic squares. Because the type-I,-II,-III and -IV magic squares are naive extensions of the magic texture of the Majorana neutrino mass matrix in Eq.(1), we separate our discussion into some parts. First, we will see the results for the type-I,-II,-III and -IV magic squares. Next, the results for type-V,-VI, ... -X magic squares are presented. Moreover, we have a discussion with the results of the recently reported T2K and NOvA tension.

#### 3.2.2. Type-I,-II,-III and -IV

We show the results from the numerical calculations for the type-I,-II,-III and -IV magic squares in Tables 1 - 3 as well as Figures 1 and 2.

Table 1 shows that the minimum and maximum values of the magic indices of type-I, -II, -III and type-IV magic squares for the Dirac flavor neutrino mass matrix. We recall that the small magic index of a matrix means the matrix is much compatible with the magic square. We note the following three points:

- The top row in the Table 1 shows that the minimum of the type-I magic index are  $s_1^{\min} = 0.132$  and  $s_1^{\min} = 0.136$  for NO and IO, respectively. Thus, the exact magic square (type-I magic square) is hardly realized for the Dirac flavor neutrino mass matrix.

Table 1. Minimum and maximum values of magic index for the type-I,-II,-III and -IV magic squares.

type	magic index	NO	IO
I	$s_I^{\min}$	<b>0.132</b>	<b>0.136</b>
	$s_I^{\max}$	0.783	0.462
II	$s_{II}^{\min}$	0.102	0.107
	$s_{II}^{\max}$	0.874	0.504
III	$s_{III}^{\min}$	0.0729	0.0956
	$s_{III}^{\max}$	0.739	0.476
IV	$s_{IV}^{\min}$	<b>0.0593</b>	<b>0.0888</b>
	$s_{IV}^{\max}$	0.832	0.525

Table 2. The sums  $S_1, S_2, \dots, S_6, T, T'$  of the type-I, -II, -III and type-IV magic squares for the Dirac flavor neutrino mass matrix in the unit of eV. The upper (lower) half of the table shows the sums in the case of NO (IO). For each type of magic squares, the upper (lower) row shows the sums for  $s_{\min}$  ( $s_{\max}$ ).

NO									
type	$s$	$S_1$	$S_2$	$S_3$	$S_4$	$S_5$	$S_6$	$T'$	$T$
I	$s_I^{\min}$	0.117	0.133	0.139	0.120	0.130	0.138	<b>0.0971</b>	<b>0.158</b>
	$s_I^{\max}$	0.0128	0.0387	0.0433	0.00166	0.0144	0.0788	0.0126	0.0436
II	$s_{II}^{\min}$	0.117	0.135	0.137	0.122	0.129	0.139	<b>0.100</b>	-
	$s_{II}^{\max}$	0.0129	0.0383	0.0432	0.00168	0.0145	0.0782	0.0123	-
III	$s_{III}^{\min}$	0.118	0.137	0.136	0.123	0.129	0.139	-	0.149
	$s_{III}^{\max}$	0.0129	0.0387	0.0432	0.00163	0.0144	0.0788	-	0.0434
IV	$s_{IV}^{\min}$	0.118	0.137	0.136	0.123	0.129	0.139	-	-
	$s_{IV}^{\max}$	0.0127	0.0389	0.0432	0.00166	0.0144	0.0788	-	-
IO									
type	$s$	$S_1$	$S_2$	$S_3$	$S_4$	$S_5$	$S_6$	$T'$	$T$
I	$s_I^{\min}$	0.129	0.126	0.138	0.137	0.148	0.107	<b>0.105</b>	<b>0.160</b>
	$s_I^{\max}$	0.0677	0.0451	0.0529	0.0798	0.0843	0.00156	0.0406	0.0619
II	$s_{II}^{\min}$	0.128	0.132	0.133	0.138	0.147	0.109	<b>0.107</b>	-
	$s_{II}^{\max}$	0.0694	0.0462	0.0543	0.0820	0.0864	0.00155	0.0414	-
III	$s_{III}^{\min}$	0.128	0.131	0.134	0.140	0.146	0.108	-	0.150
	$s_{III}^{\max}$	0.0683	0.0429	0.0559	0.0782	0.0873	0.00158	-	0.0723
IV	$s_{IV}^{\min}$	0.127	0.133	0.132	0.137	0.147	0.109	-	-
	$s_{IV}^{\max}$	0.0677	0.0430	0.0552	0.0777	0.0865	0.00163	-	-

- The smallest minimum magic index for NO(IO) is obtained in the case of type-IV as 0.0593 (0.0888). Thus, if we relax the requirement of the magic squares from exact magic square (type-I) to relatively rough magic square (type-IV), some parts of the nature of the magic square are appeared for the Dirac flavor neutrino mass matrix.
- The magic squares prefer the normal mass ordering rather than the inverted mass ordering.

Table 2 shows the sums  $S_1, S_2, \dots, S_6, T, T'$  of the type-I, -II, -III and type-IV magic squares for the Dirac flavor neutrino mass matrix in the unit of eV. The upper (lower) half of the Table 2 shows the sums in the case of NO (IO). For each

Table 3. The neutrino parameters  $m_i, \theta_{ij}, \delta$  of the type-I, -II, -III and type-IV magic squares for the Dirac flavor neutrino mass matrix. The upper (lower) half of the table shows the sums in the case of NO (IO). For each type of magic squares, the upper (lower) row shows the sums for  $s_{\min}$  ( $s_{\max}$ )

NO								
type	$s$	$m_1$ [eV]	$m_2$ [eV]	$m_3$ [eV]	$\theta_{12}/^\circ$	$\theta_{23}/^\circ$	$\theta_{13}/^\circ$	$\delta/^\circ$
I	$s_I^{\min}$	0.0745	0.0750	0.0897	36.12	51.19	8.851	183.9
	$s_I^{\max}$	0.00104	0.00834	0.0511	33.14	41.39	8.400	345.7
II	$s_{II}^{\min}$	0.0746	0.0750	0.0894	35.56	41.17	8.964	181.4
	$s_{II}^{\max}$	0.00105	0.00838	0.0507	34.92	41.12	8.270	345.9
III	$s_{III}^{\min}$	0.0748	0.0754	0.0899	36.20	51.10	8.866	340.2
	$s_{III}^{\max}$	0.00101	0.00832	0.0511	35.43	41.48	8.277	336.7
IV	$s_{IV}^{\min}$	0.0751	0.0756	0.0899	35.88	51.17	8.980	354.5
	$s_{IV}^{\max}$	0.00104	0.00832	0.0512	32.88	41.51	8.294	325.1
IO								
type	$s$	$m_1$ [eV]	$m_2$ [eV]	$m_3$ [eV]	$\theta_{12}/^\circ$	$\theta_{23}/^\circ$	$\theta_{13}/^\circ$	$\delta/^\circ$
I	$s_I^{\min}$	0.0852	0.0856	0.0691	36.21	51.20	8.982	205.1
	$s_I^{\max}$	0.0487	0.0494	0.00101	35.50	51.08	8.619	343.9
II	$s_{II}^{\min}$	0.0852	0.0856	0.0701	33.23	41.41	8.881	205.3
	$s_{II}^{\max}$	0.0500	0.0506	0.00101	35.66	51.10	8.822	347.4
III	$s_{III}^{\min}$	0.0851	0.0855	0.0699	35.74	50.98	8.947	343.5
	$s_{III}^{\max}$	0.0498	0.0506	0.00102	31.62	51.16	8.594	210.3
IV	$s_{IV}^{\min}$	0.0852	0.0857	0.0701	32.25	48.50	8.906	329.1
	$s_{IV}^{\max}$	0.0494	0.0500	0.00106	32.14	50.68	8.959	208.5

type of magic squares, the upper (lower) row shows the sums for  $s_{\min}$  ( $s_{\max}$ ). We note the following point:

- The sum of the diagonal elements  $T'$  or  $T$  tends to differ from other sums in the type-I and type-II. This character of  $T'$  or  $T$  yields the large magic index (deviation from the magic square).

Table 3 shows the neutrino parameters  $m_i, \theta_{ij}, \delta$  of the type-I, -II, -III and type-IV magic squares for the Dirac flavor neutrino mass matrix. As same as Table 2, the upper (lower) half of the Table 3 shows the sums in the case of NO (IO). For each type of magic squares, the upper (lower) row shows the sums for  $s_{\min}$  ( $s_{\max}$ ). The following ranges of the neutrino parameters are roughly favored for the magic squares:

$$\begin{aligned}
 m_i/\text{eV} &\sim 0.07 - 0.09, \\
 \theta_{12}/^\circ &\sim 36, \\
 \theta_{23}/^\circ &\sim 51, (\text{for type - I, -III, -IV}), \quad \sim 41, (\text{for type - II}), \\
 \theta_{13}/^\circ &\sim 8.9 \\
 \delta/^\circ &\sim 181 - 184, (\text{for type - I, -II}), \quad \sim 340, (\text{for type - III, IV}), \quad (34)
 \end{aligned}$$

for NO and

$$\begin{aligned}
 m_i/\text{eV} &\sim 0.07 - 0.09, \\
 \theta_{12}/^\circ &\sim 33 - 36, \\
 \theta_{23}/^\circ &\sim 51, (\text{for type - I, -III, -IV}), \quad \sim 41, (\text{for type - II}), \\
 \theta_{13}/^\circ &\sim 8.9 \\
 \delta/^\circ &\sim 205, (\text{for type - I, -II}), \quad \sim 329 - 344, (\text{for type - III, IV}),
 \end{aligned} \tag{35}$$

for IO.

Figure 1 and Figure 2 show that the dependence of the neutrino parameters  $m_i, \theta_{ij}, \delta$  on the magic index  $s$  in the case of NO and IO, respectively. We note the following four points:

- The large neutrino masses yield small magic indices (the large masses are favorable for magic squares).
- The minimum of  $s_I, s_{II}$  and  $s_{III}$  for type-I, -II and -III are obtained with large  $\theta_{12}, \theta_{23}$  and  $\theta_{13}$ .
- The minimum of  $s_I$  and  $s_{II}$  for type-I and type-II are obtained with small  $\delta$ .
- The minimum of  $s_{III}$  for type-III is obtained with large  $\delta$ .

for both NO and IO.

We would like to emphasize again the following remarkable result of our numerical calculations:

- All types of the magic squares prefer the normal mass ordering rather than the inverted mass ordering for the type-V,-VI, ..., -X magic squares (see Table 1).

Although the neutrino mass ordering (either NO or IO) is not determined experimentally, a global analysis shows that the preference for the normal mass ordering is mostly due to neutrino oscillation measurements.<sup>39,81,82</sup> The theoretical origin of the mass ordering of neutrinos is still big problem. There is a possibility that the origin of the normal mass ordering is the magic nature of the neutrinos. This conclusion becomes more rigid in the next subsubsection.

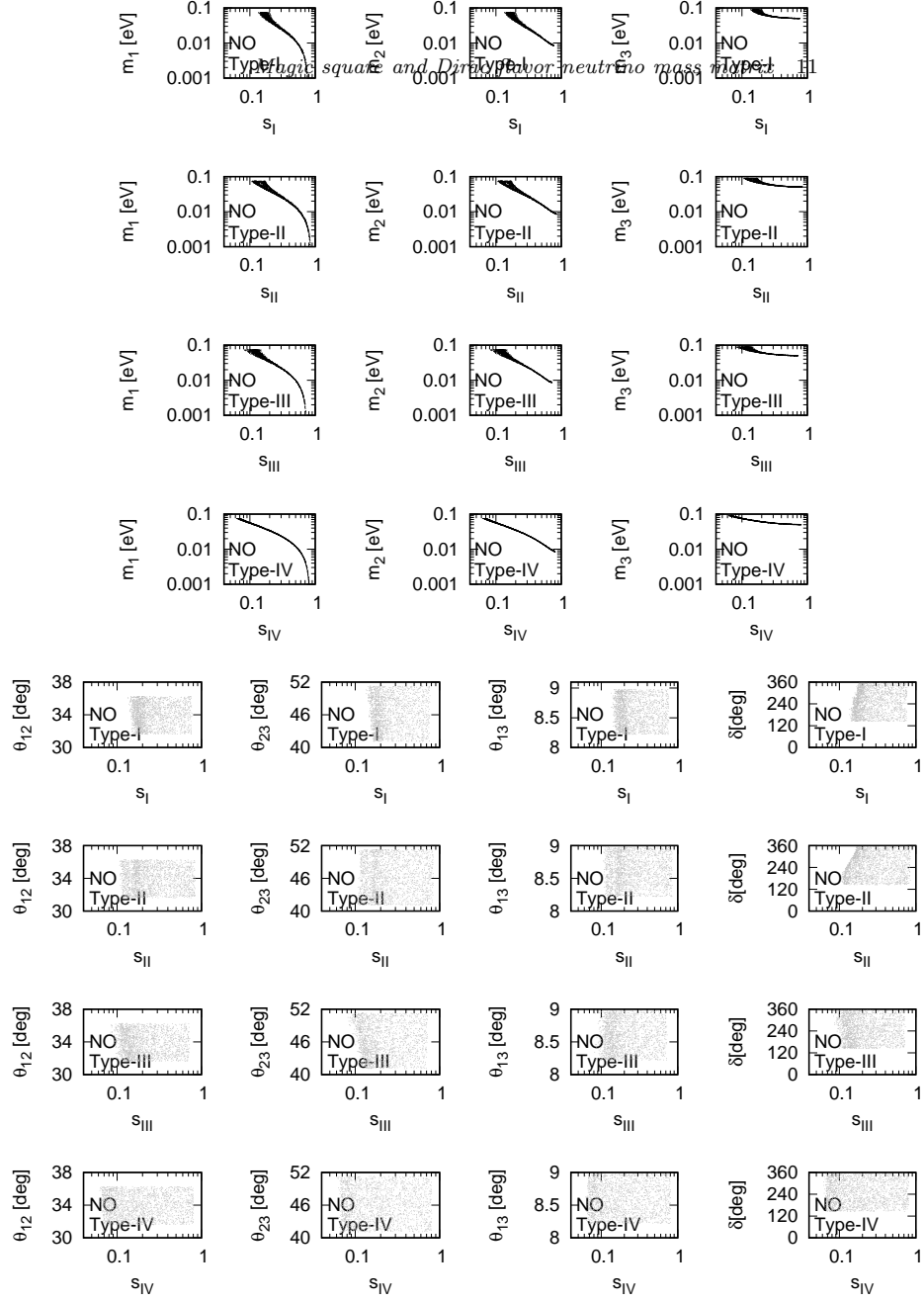


Fig. 1. Dependence of the neutrino parameters  $m_i$ ,  $\theta_{ij}$ ,  $\delta$  on the magic index  $s$  in the case of NO for the type-I,-II,-III and -IV magic squares.

12 Yuta Hyodo

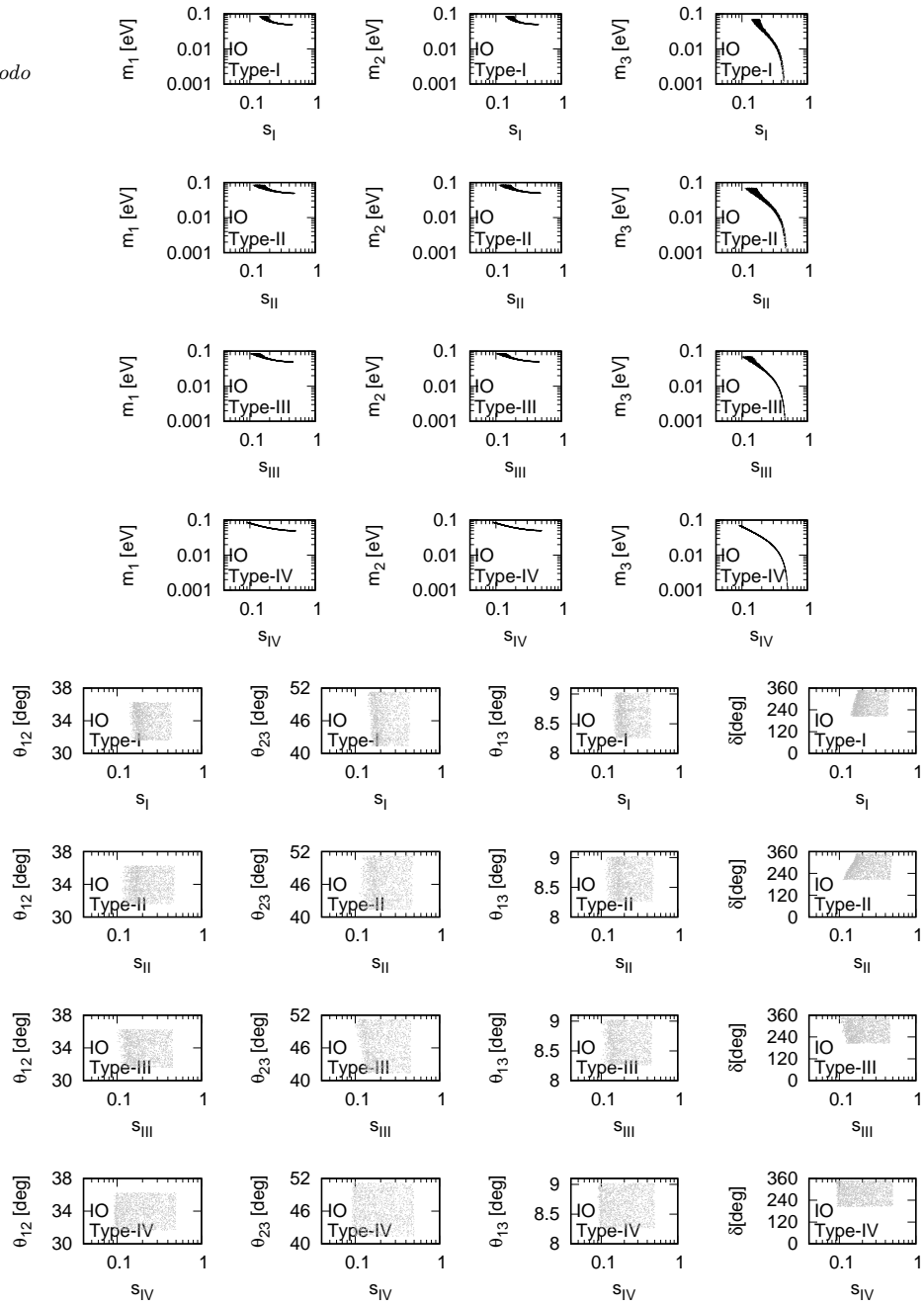


Fig. 2. Same as Figure 1 but in the case of IO.

Table 4. Minimum and maximum values of magic index for the type-V,-VI,  $\dots$ , -X magic squares.

type	magic index	NO	IO
V	$s_V^{\min}$	<b>0.133</b>	0.144
	$s_V^{\max}$	0.742	0.492
VI	$s_{VI}^{\min}$	0.140	0.143
	$s_{VI}^{\max}$	0.873	0.480
VII	$s_{VII}^{\min}$	0.138	0.144
	$s_{VII}^{\max}$	0.864	0.483
VIII	$s_{VIII}^{\min}$	0.137	0.145
	$s_{VIII}^{\max}$	0.655	0.482
IX	$s_{IX}^{\min}$	0.142	0.137
	$s_{IX}^{\max}$	0.752	0.468
X	$s_X^{\min}$	0.139	<b>0.120</b>
	$s_X^{\max}$	0.674	0.250

### 3.2.3. Type- V,-VI, $\dots$ , -X

We show the results from the numerical calculations for the type-V,-VI,  $\dots$ , -X magic squares in Tables 4 - 6 as well as Figures 3 and 6.

Table 4 shows that the minimum and maximum values of the magic indices of type-V,-VI,  $\dots$ , -X magic squares for the Dirac flavor neutrino mass matrix. Again, we recall that the small magic index of a matrix means the matrix is much compatible with the magic square. We note the following two points:

- The smallest minimum magic index for NO is obtained in the case of type-V as 0.133 and for IO is obtained in the case of type-X as 0.120. These minimum magic indices are larger than the type-IV magic indices 0.0593 (NO) and 0.0888 (IO) in Table 1. Thus, the most compatible type of magic square for Dirac neutrinos is the type-IV which is the most straight extension of the Majorana magic mass matrix texture.
- The magic squares prefer the normal mass ordering rather than the inverted mass ordering except with type-IX and type-X. According to the results shown in Tables 1 and 4, we conclude that the possibility that the origin of the normal mass ordering is the magic nature of the neutrinos becomes more rigid.

Table 5 shows the sums  $S_1, S_2, \dots, S_6, T, T'$  of the type-V,-VI,  $\dots$ , -X magic squares for the Dirac flavor neutrino mass matrix in the unit of eV. The upper (lower) half of the Table 5 shows the sums in the case of NO (IO). For each type of magic squares, the upper (lower) row shows the sums for  $s_{\min}$  ( $s_{\max}$ ). We note the following point:

- The magnitudes of the each entries in Table 5 for the type-V,-VI,  $\dots$ , -X magic squares are almost same with the magnitudes of the each entries in Table 2 for the type-I,-II,  $\dots$ , -IV magic squares.

Table 5. The sums  $S_1, S_2, \dots, S_6, T, T'$  of the type-V,-VI,  $\dots$ , -X magic squares for the Dirac flavor neutrino mass matrix in the unit of eV. The upper (lower) half of the table shows the sums in the case of NO (IO). For each type of magic squares, the upper (lower) row shows the sums for  $s_{\min}$  ( $s_{\max}$ ).

NO									
type	$s$	$S_1$	$S_2$	$S_3$	$S_4$	$S_5$	$S_6$	$T'$	$T$
V	$s_V^{\min}$	-	0.133	0.138	0.120	0.130	0.139	0.0970	0.158
	$s_V^{\max}$	-	0.0437	0.0379	0.001657	0.0147	0.0783	0.0118	0.0364
VI	$s_{VI}^{\min}$	0.117	-	0.139	0.120	0.130	0.138	0.0975	0.159
	$s_{VI}^{\max}$	0.0127	-	0.0382	0.00172	0.0143	0.0781	0.0116	0.0369
VII	$s_{VII}^{\min}$	0.118	0.133	-	0.121	0.131	0.139	0.0980	0.159
	$s_{VII}^{\max}$	0.0129	0.0431	-	0.00163	0.0142	0.0787	0.0119	0.0371
VIII	$s_{VIII}^{\min}$	0.117	0.133	0.139	-	0.130	0.139	0.0973	0.159
	$s_{VIII}^{\max}$	0.0129	0.0431	0.0374	-	0.0143	0.0775	0.0116	0.0358
IX	$s_{IX}^{\min}$	0.115	0.131	0.137	0.118	-	0.137	0.0954	0.156
	$s_{IX}^{\max}$	0.0131	0.0435	0.0378	0.00165	-	0.0781	0.0118	0.0363
X	$s_X^{\min}$	0.0117	0.133	0.138	0.119	0.123	-	0.0972	0.159
	$s_X^{\max}$	0.0126	0.0387	0.0429	0.00163	0.0146	-	0.0125	0.0431
IO									
type	$s$	$S_1$	$S_2$	$S_3$	$S_4$	$S_5$	$S_6$	$T'$	$T$
V	$s_V^{\min}$	-	0.126	0.136	0.137	0.147	0.106	0.103	0.159
	$s_V^{\max}$	-	0.0453	0.0530	0.0799	0.0847	0.00156	0.0407	0.0627
VI	$s_{VI}^{\min}$	0.128	-	0.137	0.137	0.147	0.106	0.104	0.159
	$s_{VI}^{\max}$	0.0677	-	0.0449	0.0779	0.0865	0.00159	0.0421	0.0713
VII	$s_{VII}^{\min}$	0.129	0.127	-	0.138	0.148	0.108	0.105	0.161
	$s_{VII}^{\max}$	0.0684	0.0456	-	0.0806	0.0854	0.00168	0.0409	0.0631
VIII	$s_{VIII}^{\min}$	0.128	0.126	0.137	-	0.147	0.107	0.103	0.159
	$s_{VIII}^{\max}$	0.0668	0.0528	0.0440	-	0.0853	0.00166	0.0420	0.0709
IX	$s_{IX}^{\min}$	0.128	0.126	0.137	0.137	-	0.107	0.104	0.160
	$s_{IX}^{\max}$	0.0678	0.0449	0.0532	0.0801	-	0.00154	0.0408	0.0612
X	$s_X^{\min}$	0.121	0.119	0.129	0.130	0.140	-	0.0989	0.151
	$s_X^{\max}$	0.0681	0.0458	0.0531	0.0802	0.0850	-	0.0407	0.0629

Table 6 shows the neutrino parameters  $m_i, \theta_{ij}, \delta$  of the type-V,-VI,  $\dots$ , -X magic squares for the Dirac flavor neutrino mass matrix. As same as Table 5, the upper (lower) half of the Table 6 shows the sums in the case of NO (IO). For each type of magic squares, the upper (lower) row shows the sums for  $s_{\min}$  ( $s_{\max}$ ). The following ranges of the neutrino parameters are roughly favored for the magic squares:

$$\begin{aligned}
 m_i/\text{eV} &\sim 0.07 - 0.09, \\
 \theta_{12}/^\circ &\sim 36, \\
 \theta_{23}/^\circ &\sim 51, \\
 \theta_{13}/^\circ &\sim 8.9, \\
 \delta/^\circ &\sim 165 - 180,
 \end{aligned} \tag{36}$$

Table 6. The neutrino parameters  $m_i$ ,  $\theta_{ij}$ ,  $\delta$  of the type-V,-VI, ..., -X magic squares for the Dirac flavor neutrino mass matrix. The upper (lower) half of the table shows the sums in the case of NO (IO). For each type of magic squares, the upper (lower) row shows the sums for  $s_{\min}$  ( $s_{\max}$ )

NO								
type	$s$	$m_1$ [eV]	$m_2$ [eV]	$m_3$ [eV]	$\theta_{12}/^\circ$	$\theta_{23}/^\circ$	$\theta_{13}/^\circ$	$\delta/^\circ$
V	$s_V^{\min}$	0.0743	0.0748	0.0898	36.25	51.24	8.914	170.7
	$s_V^{\max}$	0.00102	0.00858	0.0509	34.18	51.19	8.377	330.6
VI	$s_{VI}^{\min}$	0.0746	0.0752	0.0895	35.97	51.23	8.972	180.6
	$s_{VI}^{\max}$	0.00107	0.00834	0.0508	33.10	50.47	8.277	340.5
VII	$s_{VII}^{\min}$	0.0750	0.0755	0.0899	36.08	51.17	8.970	172.8
	$s_{VII}^{\max}$	0.00101	0.00830	0.0510	33.27	50.16	8.576	350.4
VIII	$s_{VIII}^{\min}$	0.0748	0.0753	0.0897	36.20	50.77	8.872	164.8
	$s_{VIII}^{\max}$	0.00102	0.00839	0.0504	34.27	51.25	8.457	351.8
IX	$s_{IX}^{\min}$	0.0734	0.0739	0.0889	36.23	51.12	8.711	183.0
	$s_{IX}^{\max}$	0.00101	0.00859	0.0508	34.63	51.10	8.438	335.8
X	$s_X^{\min}$	0.0743	0.0748	0.0889	36.05	51.05	8.959	182.9
	$s_X^{\max}$	0.00104	0.00844	0.0506	31.78	41.71	8.361	356.4
IO								
type	$s$	$m_1$ [eV]	$m_2$ [eV]	$m_3$ [eV]	$\theta_{12}/^\circ$	$\theta_{23}/^\circ$	$\theta_{13}/^\circ$	$\delta/^\circ$
V	$s_V^{\min}$	0.0843	0.0847	0.0689	36.07	50.78	8.825	208.8
	$s_V^{\max}$	0.0489	0.0496	0.00101	34.82	51.06	8.795	341.3
VI	$s_{VI}^{\min}$	0.0847	0.0851	0.0689	36.10	51.06	8.865	205.5
	$s_{VI}^{\max}$	0.0494	0.0501	0.00103	31.80	41.88	8.847	343.6
VII	$s_{VII}^{\min}$	0.0853	0.0857	0.0696	35.97	50.76	9.009	206.9
	$s_{VII}^{\max}$	0.0493	0.05000	0.00109	34.86	51.29	8.918	342.4
VIII	$s_{VIII}^{\min}$	0.0846	0.0851	0.0689	35.92	50.93	9.015	217.0
	$s_{VIII}^{\max}$	0.0487	0.0494	0.00107	31.68	41.45	8.480	340.9
IX	$s_{IX}^{\min}$	0.0848	0.0853	0.0694	35.91	51.11	8.835	206.7
	$s_{IX}^{\max}$	0.0486	0.0494	0.00100	36.14	51.18	8.435	347.2
X	$s_X^{\min}$	0.0805	0.0810	0.0643	36.19	50.89	8.895	207.8
	$s_X^{\max}$	0.0491	0.0498	0.00120	35.04	50.84	8.858	346.7

for NO and

$$\begin{aligned}
 m_i/\text{eV} &\sim 0.07 - 0.085, \\
 \theta_{12}/^\circ &\sim 36, \\
 \theta_{23}/^\circ &\sim 51, \\
 \theta_{13}/^\circ &\sim 8.8 - 9.0 \\
 \delta/^\circ &\sim 205 - 217,
 \end{aligned} \tag{37}$$

for IO. In comparison with the type-I, -II, ..., -IV magic squares, the variance of each neutrino parameters is small in the case of type-V,-VI, ..., -X magic squares.

Figure 3 and Figure 4 show that the dependence of the neutrino parameters  $m_i$ ,  $\theta_{ij}$ ,  $\delta$  on the magic index  $s$  in the case of NO. Figure 5 and Figure 6 show the same as Figure 3 and Figure 4 but in the case of IO. We note the following two points:

- The large neutrino masses yield small magic indices (the large masses are favorable for magic squares).

Table 7. The mixing angle  $\theta_{23}$  and the Dirac CP phase  $\delta$  for minimum magic index of the type-I, -II,  $\dots$ , -X magic squares for the Dirac flavor neutrino mass matrix with NO. The symbol “O” (“ $\times$ ”) means the corresponding case is favorable (unfavorable) with recent T2K or NOvA data.

	I	II	III	<b>IV</b>	V	VI	VII	VIII	IX	X
$s_i^{\min}$	0.132	0.102	0.0729	<b>0.0593</b>	0.133	0.140	0.138	0.137	0.142	0.139
$\theta_{23}/^\circ$	51.19	41.17	51.10	<b>51.17</b>	51.24	51.23	51.17	50.77	51.12	51.05
$\delta/^\circ$	183.9	181.4	340.2	<b>354.5</b>	170.7	180.6	172.8	164.8	183.0	182.9
T2K	O	$\times$	O	<b>O</b>	$\times$	O	$\times$	$\times$	O	O
NOvA	$\times$	$\times$	$\times$	$\times$	O	$\times$	O	O	$\times$	$\times$

- The minimum of magic index  $s_i$  ( $i = V, VI, \dots, X$ ) is obtained with large  $\theta_{12}$ ,  $\theta_{23}$  and  $\theta_{13}$  as well as with small  $\delta$ .

for both NO and IO.

### 3.2.4. T2K and NOvA tension

Recently, T2K and NOvA reported a tension in the measurement of  $\delta$  and  $\sin^2 \theta_{23}$  for the normal mass ordering of neutrinos.<sup>83,84</sup> Both experiments favor the upper octant of  $\theta_{23}$ ; however, the T2K data shows  $\delta > \pi$  against the NOvA result  $\delta < \pi$ . Now, we have a discussion with the results of the latest T2K and NOvA experiments.

Table 7 shows the mixing angle  $\theta_{23}$  and the Dirac CP phase  $\delta$  for minimum magic index of the type-I, -II,  $\dots$ , -X magic squares for the Dirac flavor neutrino mass matrix with NO. The symbol “O” (“ $\times$ ”) means the corresponding case is favorable (unfavorable) with recent T2K or NOvA data.

Since the most compatible type of magic square is the type-IV (which has the smallest minimum magic index  $s_{IV}^{\min} = 0.0593$ ), it seems that the T2K result is more favorable than the NOvA result in the context of the magic square.

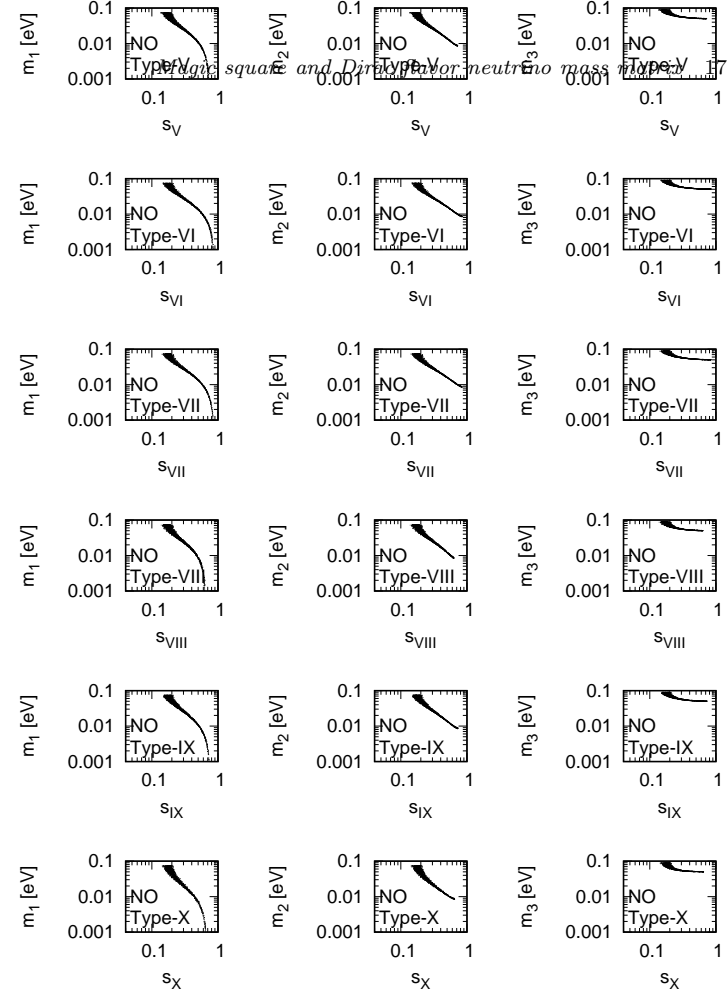


Fig. 3. Dependence of the neutrino mass  $m_i$  on the magic index  $s$  in the case of NO for the type-V,-VI, ..., -X magic squares.

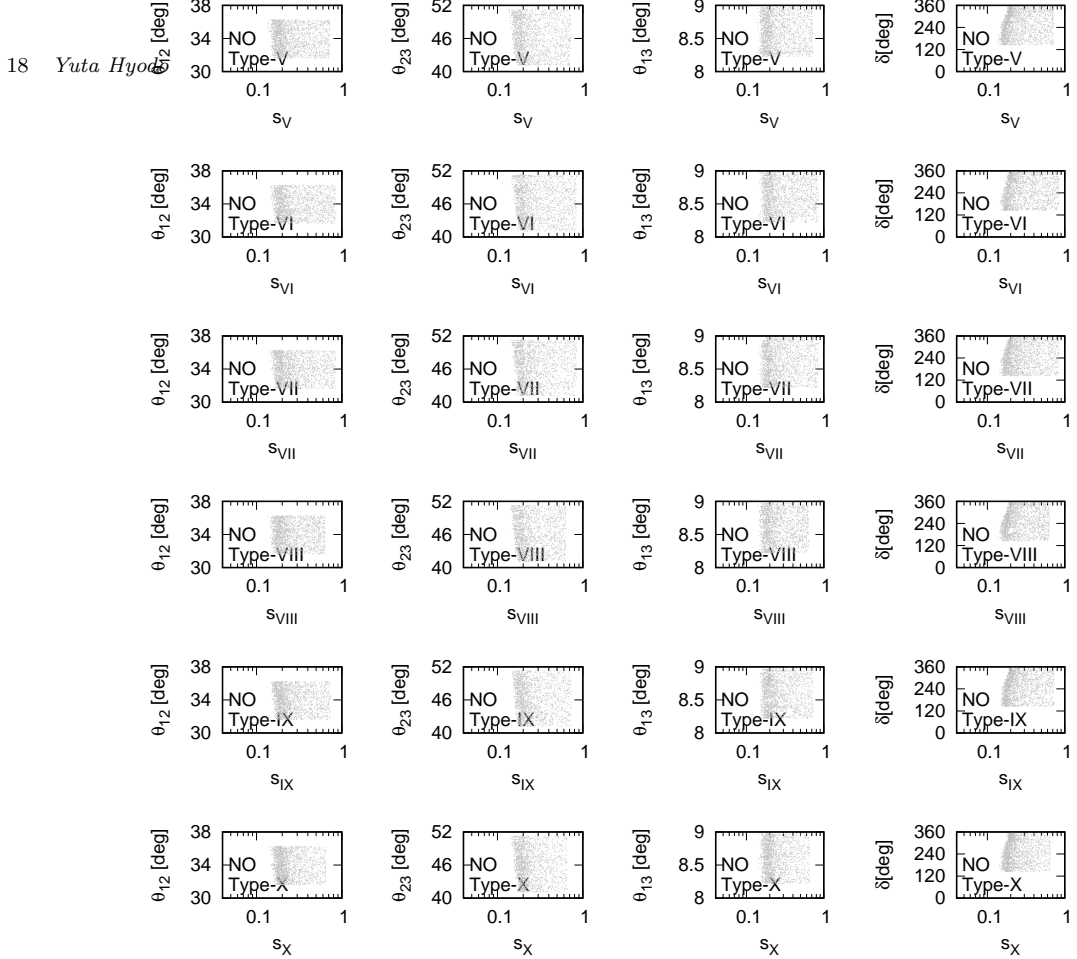


Fig. 4. Dependence of the neutrino mixing angles and phase  $\theta_{ij}, \delta$  on the magic index  $s$  in the case of NO for the type-V, -VI, ..., -X magic squares.

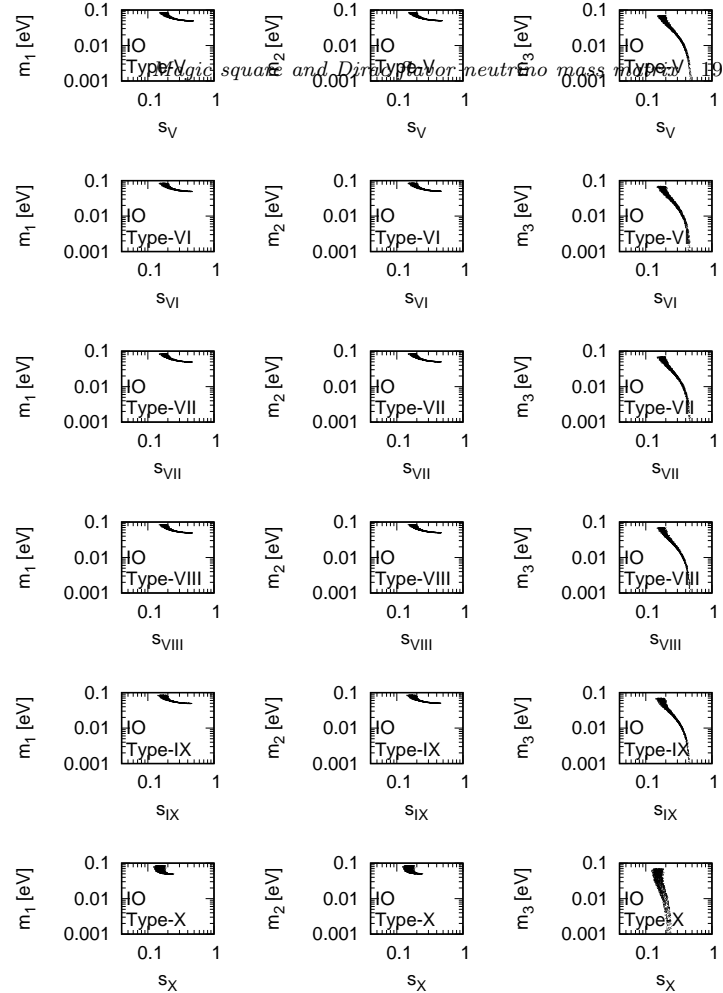


Fig. 5. Same as Figure 3 but in the case of IO.

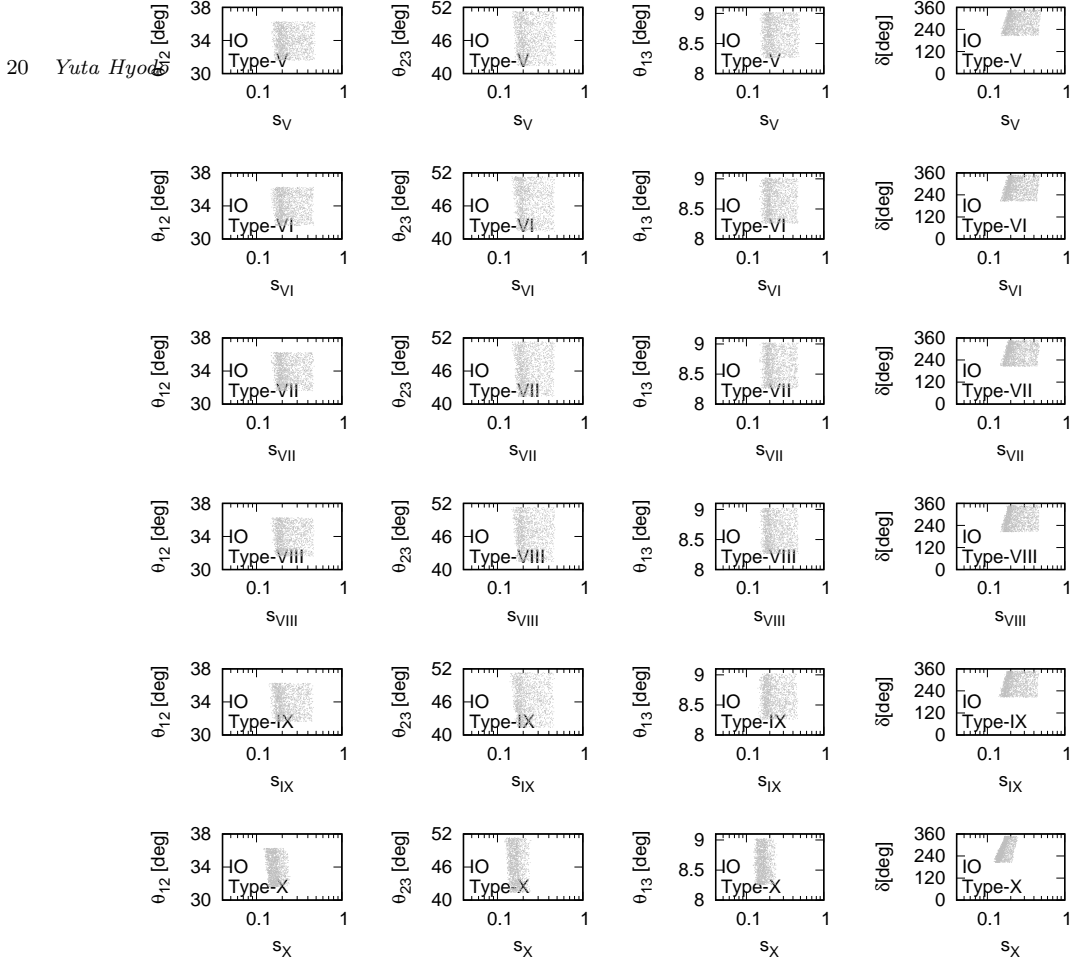


Fig. 6. Same as Figure 4 but in the case of IO.

#### 4. Summary

The magic texture is one of the successful textures of the flavor neutrino mass matrix for the Majorana type neutrinos. The name “magic” is inspired by the nature of the magic square. In this paper, we have estimated the compatibility of the magic square with the Dirac, instead of the Majorana, flavor neutrino mass matrix by numerical calculations. We have shown that some parts of the nature of the magic square are appeared approximately in the Dirac flavor neutrino mass matrix and the magic squares prefer the normal mass ordering rather than the inverted mass ordering for the Dirac neutrinos. Moreover, we have mentioned about the recently reported a tension between T2K and NOvA experiments. It turned our that the T2K result is more favorable than the NOvA result in the context of the magic square.

Finally, we would like to comment about Eq.(33). In this paper, we have estimated the compatibility of the magic square with the real matrix in Eq.(33) instead of the complex Dirac mass matrix in Eq.(27). This approach may be enough as a first step of the study about the relation between the magic square and the Dirac flavor neutrino mass matrix; however, if we estimate the compatibility of the magic square with the complex Dirac mass matrix in Eq.(27) by an appropriate method, the results may be modified. A detailed analysis of this topic will be found in our future study.

#### References

1. S. F. King, J. Phys. G **42**, 123001 (2015).
2. F. Feruglio and A. Romanino, “Neutrino Flavour Symmetries”, arXiv:1912.06028 (Dec 2019).
3. P. F. Harrison, D. H. Perkins, and W. G. Scott, Phys. Lett. B **530**, 167 (2002).
4. Z. -z. Xing, Phys. Lett. B **533**, 85 (2002).
5. P. F. Harrison and W. G. Scott, Phys. Lett. B **535**, 163 (2002).
6. M. S. Berger and K. Siyeon, Phys. Rev. D **64**, 053006 (2001).
7. P. H. Frampton, S. L. Glashow, and D. Marfatia, Phys. Lett. B **536**, 79 (2002).
8. Z. -z. Xing, Phys. Lett. B **530**, 159 (2002).
9. Z. -z. Xing, Phys. Lett. B **539**, 85 (2002).
10. A. Kageyama, S. Kaneko, N. Shimoyana, and M. Tanimoto, Phys. Lett. B **538**, 96 (2002).
11. Z. -z. Xing, Phys. Rev. D **69**, 013006 (2004).
12. W. Grimus, A. S. Joshipura, L. Lavoura, and M. Tanimoto, Eur. Phys. J. C **36**, 227 (2004).
13. C. I. Low, Phys. Rev. D **70**, 073013 (2004).
14. C. I. Low, Phys. Rev. D **71**, 073007 (2005).
15. W. Grimus and L. Lavoura, J. Phys. G **31**, 693 (2005).
16. S. Dev, S. Kumar, S. Verma, and S. Gupta, Phys. Rev. D **76**, 013002 (2007).
17. Z. -z. Xing and S. Zhou, Phys. Lett. B **679**, 249 (2009).
18. H. Fritzsch, Z. -z. Xing, and S. Zhou, J. High Energy Phys. **09**, 083 (2011).
19. S. Kumar, Phys. Rev. D **84**, 077301 (2011).
20. S. Dev, S. Gupta, and R. R. Gautam, Phys. Lett. B **701**, 605 (2011).

21. T. Araki, J. Heeck, and J. Kubo, *J. High Energy Phys.* **07**, 083 (2012).
22. P. Ludle, S. Morisi, and E. Peinado, *Nucl. Phys. B* **857**, 411 (2012).
23. E. Lashin and N. Chamoun, *Phys. Rev. D* **85**, 113011 (2012).
24. K. Deepthi, S. Gollu, and R. Mohanta, *Eur. Phys. J. C* **72**, 1888 (2012).
25. D. Meloni and G. Blankenburg, *Nucl. Phys. B* **867**, 749 (2013).
26. D. Meloni, A. Meroni, and E. Peinado, *Phys. Rev. D* **89**, 053009 (2014).
27. S. Dev, R. R. Gautam, L. Singh, and M. Gupta, *Phys. Rev. D* **90**, 013021 (2014).
28. R. G. Felipe and H. Serodio, *Nucl. Phys. B* **886**, 75 (2014).
29. P. O. Ludl and W. Grimus, *J. High Energy Phys.* **07**, 090 (2014).
30. L. M. Cebola, D. E. Costa, and R. G. Felipe, *Phys. Rev. D* **92**, 025005 (2015).
31. R. R. Gautam, M. Singh, and M. Gupta, *Phys. Rev. D* **92**, 013006 (2015).
32. S. Dev, L. Singh, and D. Raj, *Eur. Phys. J. C* **75**, 394 (2015).
33. T. Kitabayashi and M. Yasuè, *Phys. Rev. D* **93**, 053012 (2016).
34. S. Zhou, *Chin. Phys. C* **40**, 033102 (2016).
35. M. Singh, G. Ahuja and M. Gupta, *Prog. Theor. Exp. Phys.* **2016**, 123B08 (2016).
36. K. Bora, D. Borah and D. Dutta, *Phys. Rev. D* **96**, 075006 (2017).
37. D. M. Barreiros, R. G. Felipe and F. R. Joaquim, *Phys. Rev. D* **97**, 115016 (2018).
38. D. M. Barreiros, R. G. Felipe and F. R. Joaquim, *J. High Energy Phys.* **01**, 223 (2019).
39. F. Capozzi, E. D. Valentino and E. Lisi, A. Marrone, A. Melchiorri and A. Palazzo, *Phys. Rev. D* **101**, 116013 (2020).
40. M. Singh, *EPL* **2020**, 11002 (2020).
41. D. M. Barreiros, F. R. Joaquim and T. T. Yanagida, arXiv:2003.06332.
42. T. Fukuyama and H. Nishiura, (1997), arXiv:hep-ph/9702253.
43. C. S. Lam, *Phys. Lett. B* **507**, 214 (2001).
44. E. Ma and M. Raidal, *Phys. Rev. Lett.* **87**, 011802 (2001); Erratum *Phys. Rev. Lett.* **87**, 159901 (2001).
45. K. R. S. Balaji, W. Grimus, and T. Schwetz, *Phys. Lett. B* **508**, 301 (2001).
46. Y. Koide, H. Nishiura, K. Matsuda, T. Kikuchi, and T. Fukuyama, *Phys. Rev. D* **66**, 093006 (2002).
47. T. Kitabayashi and M. Yasue, *Phys. Rev. D* **67**, 015006 (2003).
48. Y. Koide, *Phys. Rev. D* **69**, 093001 (2004).
49. I. Aizawa, M. Ishiguro, T. Kitabayashi, and M. Yasue, *Phys. Rev. D* **70**, 015011 (2004).
50. A. Ghosal, *Mod. Phys. Lett. A* **19**, 2579 (2004).
51. R. N. Mohapatra and W. Rodejohann, *Phys. Rev. D* **72**, 053001 (2005).
52. Y. Koide, *Phys. Lett. B* **607**, 123 (2005).
53. T. Kitabayashi and M. Yasue, *Phys. Lett. B* **621**, 133 (2005).
54. N. Haba and W. Rodejohann, *Phys. Rev. D* **74**, 017701 (2006).
55. Z.-z. Xing, H. Zhang, and S. Zhou, *Phys. Lett. B* **641**, 189 (2006).
56. Y. H. Ahn, S. K. Kang, C. S. Kim, and J. Lee, *Phys. Rev. D* **73**, 093005 (2006).
57. A. S. Joshipura, *Eur. Phys. J. C* **53**, 77 (2008).
58. J. C. Gomez-Izquierdo and A. Perez-Lorenzana, *Phys. Rev. D* **82**, 033008 (2010).
59. H.-J. He and F.-R. Yin, *Phys. Rev. D* **84**, 033009 (2011).
60. H.-J. He and X.-J. Xu, *Phys. Rev. D* **86**, 111301 (2012).
61. J. C. Gomez-Izquierdo, *Eur. Phys. J. C* **77**, 551 (2017).
62. T. Fukuyama, *Prog. Theor. Exp. Phys.* **2017**, 033B11 (2017).
63. G. Altarelli and F. Feruglio, *Rev. Mod. Phys.* **82**, 2701 (2010).
64. P. F. Harrison and W. G. Scott, *Phys. Lett. B* **594**, 324 (2004).
65. C. S. Lam, *Phys. Lett. B* **640**, 260 (2006).
66. R. R. Gautam and S. Kumar, *Phys. Rev. D* **94**, 036004 (2016).
67. K. S. Chaney and S. Kumar, *J. Phys. G: Nucl. Part. Phys.* **46**, 015001 (2019).

68. S. Verma and M. Kashav, arXiv:1910.04467v2 (Jan. 2020).
69. A. Levitin, and M. Levitin, “Algorithmic Puzzles”, Oxford University Press, New York (2011).
70. C. Hagedron and W. Rodejohann, J. High Energy Phys. **07**, 034 (2005).
71. B. Pontecorvo, Sov. Phys. JETP 6 (1957) 429.
72. B. Pontecorvo, Sov. Phys. JETP 7 (1958) 172;
73. Z. Maki, M. Nakagawa and S. Sakata, Prog. Theor. Phys. **28**, 870 (1962).
74. M. Tanabashi *et al.* (Particle Data Group), Phys. Rev. D **98**, 030001 (2018).
75. I. Esteban, M. C. Gonzalez-Garcia, A. H-Cabezudo, M. Maltoni, and T. Schwetz, J. High Energy Phys. **01**, 106 (2019). See also, NuFIT webpage, <http://www.nu-fit.org>.
76. N. Aghanim, et al. (Planck Collaboration), “Planck 2018 results. VI. Cosmological parameters”, arXiv:1807.06209v2 (Sep 2019).
77. E. Giusarma, M. Gerbino, O. Mena, S. Vagnozzi, S. Ho and K. Freese, Phys. Rev. D **94**, 083522 (2016).
78. S. Vagnozzi, E. Giusarma, O. Mena, K. Freese, M. Gerbino, S. Ho and M. Lattanzi, Phys. Rev. D **96**, 123503 (2017).
79. E. Giusarma, S. Vagnozzi, S. Ho, S. Ferraro, K. Freese, R. K.-Rubio and K.-B. Luk, Phys. Rev. D **98**, 123536 (2018).
80. M. Agostini, et al., (GERDA Collaboration), Science **365**, 1445 (2019).
81. P. F. de Salas, D. V. Forero, C. A. Ternes, Tórtola and J.W.F. Valle, Phys. Lett. B **782**, 633 (2018).
82. M. G. Aartsen, et al., (IceCube-Gen2 Collaboration) and T. J. C. Bezerra, et al., (JUNO Collaboration), Phys. Rev. D **101**, 032006 (2020).
83. A. Himmel, (NOvA Collaboration), “New Oscillation Results from the NOvA Experiment”, Neutrino 2020, Fermilab (Jul. 2020). <https://conferences.fnal.gov/nu2020/>
84. P. Dunne, (T2K Collaboration), “Latest Neutrino Oscillation Results from T2K”, Neutrino 2020, Fermilab (Jul. 2020). <https://conferences.fnal.gov/nu2020/>